*Annals of Biomedical Engineering*, Vol. 32, No. 11, November 2004 (© 2004) pp. 1559–1568

# A Spatially Explicit Nanomechanical Model of the Half-Sarcomere: Myofilament Compliance Affects $Ca^{2+}$-Activation

P. BRYANT CHASE,[1] J. MICHAEL MACPHERSON,[2] and THOMAS L. DANIEL[3]

[1]Department of Biological Science and Program in Molecular Biophysics, Florida State University, Tallahassee, FL; [2]Department of Biological Sciences, Stanford University, Stanford, CA; and [3]Department of Biology, University of Washington, Seattle, WA

*(Received 11 Februaury 2004; accepted 30 July 2004)*

**Abstract—**The force exerted by skeletal muscle is modulated by compliance of tissues to which it is connected. Force of the muscle sarcomere is modulated by compliance of the myofilaments. We tested the hypothesis that myofilament compliance influences $Ca^{2+}$ regulation of muscle by constructing a computational model of the muscle half sarcomere that includes compliance of the filaments as a variable. The biomechanical model consists of three half-filaments of myosin and 13 thin filaments. Initial spacing of motor domains of myosin on thick filaments and myosin-binding sites on thin filaments was taken to be that measured experimentally in unstrained filaments. Monte-Carlo simulations were used to determine transitions around a three-state cycle for each cross-bridge and between two-states for each thin filament regulatory unit. This multifilament model exhibited less "tuning" of maximum force than an earlier two-filament model. Significantly, both the apparent $Ca^{2+}$-sensitivity and cooperativity of activation of steady-state isometric force were modulated by myofilament compliance. Activation-dependence of the kinetics of tension development was also modulated by filament compliance. Tuning in the full myofilament lattice appears to be more significant at submaximal levels of thin filament activation.

**Keywords—**Muscle, Actin filament, Myosin filament, Cross-bridge, Troponin, Tropomyosin, Calcium regulation, Force, Kinetics of tension development.

## INTRODUCTION

The sarcomere of striated muscles is a highly ordered array of proteins that efficiently converts chemical energy (MgATP) into mechanical work. Sarcomeres are composed of two types of filaments. Thick filaments consist primarily of the biological motor protein myosin (~300 molecules of myosin or 600 motor domains per thick filament).[2] The second type, thin filaments, are the "tracks" on which myosin motors move. Thin filaments are composed of ~380 actin monomers and, in vertebrate sarcomeres, the $Ca^{2+}$-regulatory proteins troponin and tropomyosin (Tm) in a ratio of one troponin plus one Tm to seven actin monomers.[17] Each troponin is a complex of three distinct subunits and is the $Ca^{2+}$-binding element in regulation of contraction. Each Tm is an $\alpha$-helical coiled-coil dimer that is physically associated not only with a troponin complex and seven actins of the structural regulatory unit, but also with adjacent Tm molecules; Tm's are connected end-to-end to form two continuous strands that coil around opposite sides of an actin filament. The sheer number of protein subunits and their interactions could lead to significant cooperativity in muscle function. Biophysical measurements confirm that this is indeed the case.[17]

The periodicity of myosin motors in thick filaments is ~15% larger than that of myosin binding sites in thin filaments. Increased $[Ca^{2+}]_i$ and the corresponding isometric tension of muscle lead to significant changes in these periodicities because of elongation of both thick and thin filaments[21,43] even though the elastic modulus of protein filaments is measured in giga-Pascals and single motor forces are measured in pico-Newtons.[16,20,22,33] These structural changes in the filaments could cause direct or apparent changes in cooperativity of muscle function. Computational models[11,31] and experimental measurements[25,29] indicate that this filament compliance can, and does, have functionally significant consequences, although the full extent of these consequences is only beginning to be understood (note that compliance is the inverse of stiffness). Daniel *et al.*[11] suggested, from modeling studies with one thick filament and one unregulated actin filament, that compliance-related realignment of myosin-binding sites on actin (CRB) could lead to "tuning" of peak isometric force—force in the model was higher at values of filament compliance near that measured experimentally. Additionally, compliance can lead to temporal tuning as well.[12] Those computational studies left open the question of whether tuning could also be present in the full three-dimensional filament lattice of the intact sarcomere. There are greater numbers of actomyosin interactions, and thus higher forces and greater filament strain, in the full filament lattice because each thick filament can interact with six actin filaments and each

Address correspondence to P. Bryant Chase, PhD, FAHA, Department of Biological Science and Program in Molecular Biophysics, Florida State University, Bio Unit One, Tallahassee, FL 32306-4370. Electronic mail: chase@bio.fsu.edu

actin filament is in turn surrounded by three thick filaments (Fig. 1). Furthermore, it raises the question of whether CRB-related tuning could influence the $Ca^{2+}$-dependence of force development when the $Ca^{2+}$-regulatory proteins troponin and Tm are present on thin filaments.

We therefore constructed a Monte-Carlo simulation immersed in a biomechanical model that incorporates: the numbers and linear spacing of myosin motors and their binding sites on actin that are found within the filament lattice of the muscle sarcomere; filament compliance; and a defined probability of activation for each myosin-binding site that simulated $Ca^{2+}$-regulation with no intrinsic cooperativity. The predictions of this modeling are three-fold. First, there is less tuning of peak force than the two-filament model, although the multifilament model with its inherently higher forces per filament is not immune to this tuning phenomenon. Second, both the apparent $Ca^{2+}$-sensitivity and cooperativity of activation of steady-state isometric force are significantly modulated by compliance in the filaments. Third, the activation-dependence of tension development kinetics is also significantly modulated by filament compliance. Portions of this work have been reported in abstract form.[9]

## MATERIALS AND METHODS

Our modeling effort is divided into three portions, each more fully detailed below. We first create a spatially explicit model of the geometry of interacting filaments that accounts for the three-dimensional packing of filaments in a muscle fiber and the spatial distribution of motor molecules and their putative binding sites. We then imbue this geometric model with mechanical characteristics that best reflect the known values for the spring constants of thin and thick filaments as well as the myosin motors. With the geometric and mechanical aspects of the model specified we then develop two kinetic models. One uses a previously developed three state model for myosin cross-bridge cycling. The other simulates $Ca^{2+}$ attachment to thin filament regulatory units (troponin–Tm) with a probabilistic model of myosin-binding site availability.

### *Geometry*

We use an extension of the model initially developed by Daniel *et al.*[11] which is based on the geometry of a half sarcomere composed of three thick filaments and a hexagonally packed array of 13 thin filaments surrounding these thick filaments (Fig. 1). The thick and thin filaments have lengths of 1.8 and 1.1 $\mu$m, respectively. Each half-thick filament is armed with 120 cross-bridges arranged in a helical pattern along the length of the filament. The spacing between collinear cross-bridges is 42.9 nm, consistent with the average spacing in vertebrate striated muscle.[19,21,43] Each thin filament has binding sites also arranged helically along its length so that a spacing of 37.3 nm between collinear binding sites faces one thick filament.[34]

A ratio of three thick filaments to 13 thin filaments does not reflect the ratio seen in a muscle fiber where the large numbers of filaments yields a ratio closer to 1:3, although this ratio may be altered by disease or pattern of muscle use.[1,39] To account for this discrepancy between a limited number of filaments in the model versus the much larger number in the filament lattice of living muscle, each of the surrounding thin filaments interacts with motor molecules from the three core thick filaments (Fig. 1(A)). For example, the central thin filament in the lattice interacts with cross-bridges from all three thick filaments. Each thick filament can, therefore, experience forces transmitted through that thin filament. However, most of the thin filaments in this lattice have binding sites that face away from one of the three thick filaments. We mapped myosin interactions onto that array in a way that creates forces on thin filaments without explicitly adding extra thick filaments to the model. For example, the thick filament labeled "1" has myosins that interact with the six thin filaments directly surrounding it as well as seven additional ones that face outward (each labeled "1" in Fig. 1(A)).

Our model is necessarily spatially explicit. As such, each binding site and each motor molecule has a unique location specified by the geometry. With the three thick filaments and 13 thin filaments we use a force balance (see below) to account for the location of 360 myosins ($m_1, m_2, \ldots m_{360}$) and 1170 thin filaments binding sites ($a_1, a_2, \ldots a_{1170}$).

### *Mechanics*

The lattice of thick and thin filaments is modeled as a three dimensional array of springs that are potentially connected by cross-bridges. The elasticity of each cross-bridge is assumed to behave linearly, with an initial spring constant of $K_{xb} = 1$ pN/nm.[42] The thin filament is modeled as a system of linear springs connecting sequential binding sites, each assigned a spring constant of $K_a = 5230$ pN/nm and a rest length $a_o = 12.33$ nm. Similarly each thick filament is modeled as a system of linear springs connecting sequential cross-bridges. The spring constant for thick filaments is $K_m = 6060$ pN/nm and each spring has a rest length of $m_o = 14.33$ nm. These spring constants, or stiffness values, are inversely related to compliance of the filament segments. We intersperse both terminologies throughout this work, with "filament compliance" often used to recognize that myofilaments are not infinitely stiff. Because we are modeling a helical arrangement of actin binding sites and myosin motors with one third the spacing between collinear sites, the spring constants used here are three times greater than those used in the one-dimensional model developed previously.[11]

We further assume that both viscous and inertial forces are negligible and no additional external forces are applied

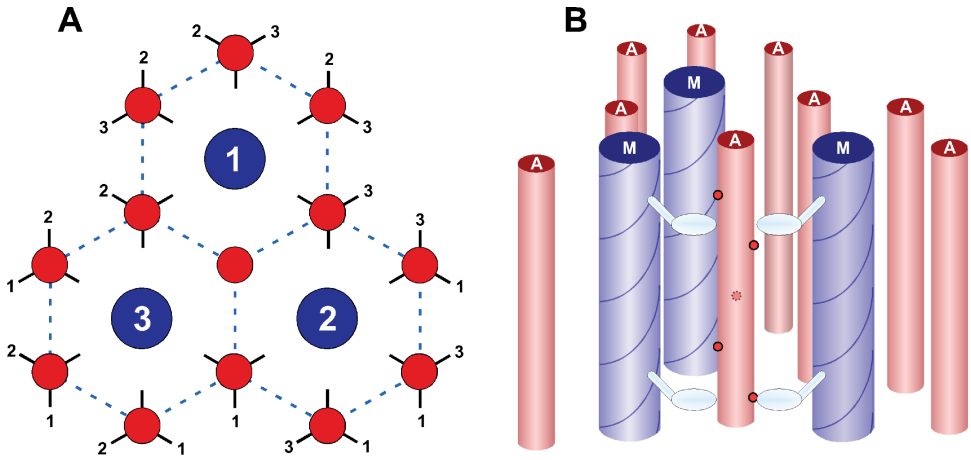


**FIGURE 1.** (A) Schematic cross-section through the muscle half-sarcomere (Z-disc to M-zone) filament lattice represented in the model. The model consists of three thick (myosin) filaments (blue, labeled 1, 2, 3), surrounded by 13 thin (actin–troponin–Tm) filaments (red) in a hexagonal lattice. Longitudinal forces in the finite element matrix (along the muscle's major axis, perpendicular to the page) are mirrored as indicated at the edges of the diagrammed region to simulate the presence of additional thick filaments in the lattice. (B) Three-dimensional representation of nodes in the finite element matrix. Thick filaments (blue) are labeled M. Thin filaments (red) are labeled A. Myosin binding sites on actin are indicated by dots. Note that only 9 of the 13 actin filaments are shown in panel B for clarity.

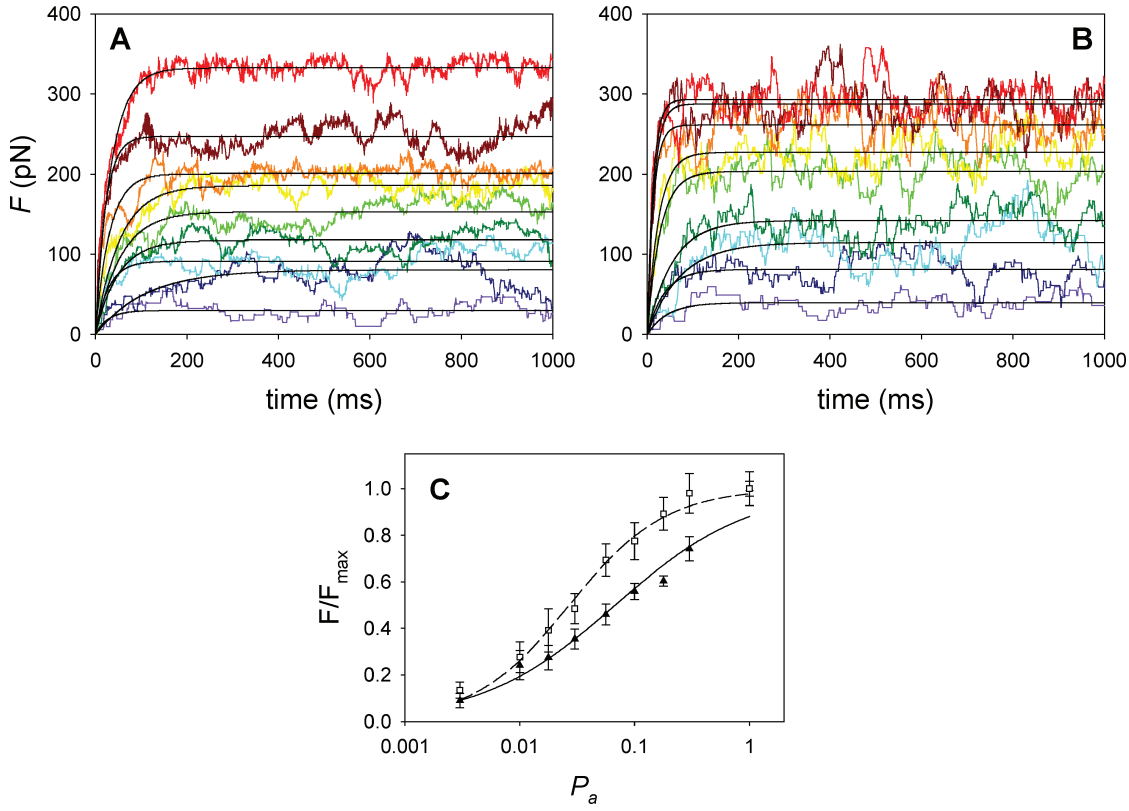


**FIGURE 2.** Example simulations of isometric force ($F(t)$). Model output for $K_{xb} = 1$ pN/nm and $K_a = 523$ pN/nm (A) or 52,300 pN/nm (B) which correspond to 10 or 1000%, respectively, of $K_a$ measured in frog skeletal muscle (5230 pN/nm; Methods). In A and B, nine separate simulations are superimposed, each at a different activation probability ($P_a = 1.0$, red; $P_a = 0.3$, dark red; $P_a = 0.178$, orange; $P_a = 0.1$, yellow; $P_a = 0.0562$, light green; $P_a = 0.03$, dark green; $P_a = 0.0178$, cyan; $P_a = 0.01$, dark blue; $P_a = 0.003$, purple). Black lines are nonlinear least squares fits to a rising mono-exponential function (Eq. (5)) for each simulation. (C) Steady-state isometric force ($F$ in Eq. (5)), normalized to $F_{max}$ ($F$ for $P_a = 1.0$), as a function of $P_a$. Solid triangles and solid line are from panel A ($K_a = 523$ pN/nm), and open squares and dashed line are from panel B ($K_a = 52{,}300$ pN/nm). Error bars indicate SD from force simulations between $t = 300$–1000 ms (note that regression SE for $F$ was <6% of SD shown). Lines were drawn according to the nonlinear least squares regressions of Eq. (6) to the points shown.

to the lattice. With these assumptions, we develop an instantaneous force balance for the *i*th bound myosin molecule and the *j*th thin filament binding site:

$$K_m(m_{i+1} - m_i - m_o) + K_{xb,i}(a_j - m_i - x_o) - K_m(m_i - m_{i-1} - m_o) = 0 \quad (1)$$

$$K_a(a_{j+1} - a_j - a_o) - K_{xb,i}(a_j - m_i - x_o) - K_a(a_{j+1} - a_{j-1} - a_o) = 0. \quad (2)$$

The equations above form a coupled system of linear equations for the locations $m_i$ and $a_i$. Constructing a single vector for all locations ($\mathbf{X} = m_1, m_2, \ldots m_{360}, a_1, a_2, \ldots a_{1170}$), a matrix for all spring constants ($\mathbf{K}$), and a vector defined by the constant products of spring constants and rest lengths ($\mathbf{V}$) yields a linear system that is solved by inversion:

$$\mathbf{X} = \mathbf{K}^{-1} \cdot \mathbf{V} \quad (3)$$

The matrix is sparse and conditioning it assists in the run time. The key to solving this system lies in the construction of the correct matrix of spring constants. With no bound myosin molecules, there are no contributions of the $K_{xb,i}$ elements into the matrix. Upon binding, however, the *i*th myosin motor interacts with the *j*th binding site with that spring constant. Cross-bridge (or external) forces act to distort nodes in the position matrix only in the axial dimension; radial forces and changes in filament lattice spacing are not considered in this model although they are known to be a significant physiological and experimental parameters.[32]

### *Kinetics*

As in Daniel *et al.*,[11] we use a three state model to represent probabilities for cross-bridge attachment to, or detachment from, thin filament binding sites, or transition between attached states. By this scheme, a motor molecule may reside in a detached state, a weakly attached state, or a strongly attached state. These follow from a range of simplified models of acto–myosin interaction.[11,17] The likelihood for attachment depends upon the distance to a binding site and the availability of that site. The former is determined by the geometry and mechanics of the lattice with an exponential decline in attachment likelihood with increasing distance[11]; distances greater than about 2 nm have attachment probabilities that fall below 0.2. The availability of a binding site is determined by intracellular $Ca^{2+}$ concentration. To model availability, we define an activation probability ($P_a$) which determines the fraction of binding sites we define as available. For example, with $P_a = 0.5$, we randomly assign half of the binding sites as available (see below). We have intentionally omitted interactions between regulatory units in these computations to determine the effects of compliance in the absence of this additional complexity. Rather than modeling the specific $Ca^{2+}$ association and dissociation kinetics of troponin, which in actual thin filaments are convolved with the kinetics of conformational changes in the regulatory proteins, we use this simpler approach to examine how filament compliance in the context of partial activation determines force production in muscle.

Modeling cross-bridge transitions between weakly and strongly bound states, as well as their detachment likelihood, follows directly from Daniel *et al.*,[11] and is consistent with the constraint of free energy available from ATP hydrolysis. In all of these state transitions, the distortion of the cross-bridge is a critical determinant of functional performance. In addition, intracellular free phosphate concentration (taken here to be 2 mM) determines these transitions. Consistent with most models of cross-bridge cycling, we assume each detachment event coincides with the binding and hydrolysis of one ATP molecule.

### *Programming Approach*

All of the programs are written in MATLAB (The MathWorks). We use two Monte-Carlo processes, one for simulating binding site availability and the other for simulating cross-bridge state transitions. For any specified activation probability, the simulation is initiated with all cross-bridges detached (i.e., there is no force generated). At the first time step, the availability of each thin filament binding site is determined by one Monte-Carlo process in which we assign the site a uniform random number on [0, 1] and compare that number with $P_a$. If it is less than $P_a$, the site is available. Thus with $P_a = 1$ all sites are available.

The second Monte-Carlo process proceeds for this first and all future time steps and is applied to all of the cross-bridges. With all cross-bridges initially unbound, entries into the matrix of spring constants have a value of zero for any $K_{xb}$. Each cross-bridge is assigned a uniform random number on [0, 1] at every time step. That random number is used along with the transition probabilities to determine in which state a cross-bridge will reside. For unbound cross-bridges, the distance to the nearest binding site is used to compute the probability of weak attachment. If that probability is less than a random number assigned to that cross-bridge, attachment occurs; otherwise it remains unattached. The likelihood of proceeding directly from an unbound state to one that is strongly bound is negligible. Thus this part of the simulation requires a single probability comparison.

A weakly bound cross-bridge could remain in that state, revert to an unbound state, or proceed forward into the strongly bound state. Similarly, strongly bound cross-bridges could revert to the weakly bound state, remain strongly bound, or detach. Thus for these two states we formulate a two-tailed probability comparison. With $R$ as the random number assigned to each cross-bridge and $P_f$ and $P_r$ defining, respectively, the forward and reverse transition probabilities the state of each cross-bridge follows

from the truth table:

$$\begin{aligned} &\text{Reverse} : 0 \le R < P_{\mathrm{r}} \\ &\text{No change} : P_{\mathrm{r}} \le R \le (1 - P_{\mathrm{f}}) \\ &\text{Forward} : (1 - P_{\mathrm{f}}) < R \le 1). \end{aligned} \tag{4}$$

At the end of each time step, the state of each cross-bridge is determined from the above. Those that have become attached require the addition of cross-bridge spring constants to the portions of the spring constant matrix corresponding to their entries. Those that have become detached require that their cross-bridge spring constants take on a value of 0. Those cross-bridges that have undergone a transition from the weakly- to strongly-bound state require a modification to the extent of cross-bridge distortion that corresponds to the unstrained state ($x_{\mathrm{o}}$). In this case, the release of phosphate corresponds to a decrease in $x_{\mathrm{o}}$ of 7 nm.[11]

Once the states are known and the appropriate spring constants are placed in their respective locations in the matrix, we solve for the vector of locations using Eq. (3). These locations combined with the force balance above gives us the total force borne by each filament. We use the sum of the forces borne by the three thick filaments to compute the force produced at each instant in time. We use a step size of 1 ms and a total simulation time of 500–1000 steps. Because of the stochastic nature of Monte-Carlo processes, we repeat each simulation up to 100 times to acquire reasonable means and standard deviations, as detailed in Results.

The result of each 500–1000 ms simulation of force development was fit using nonlinear least squares regression to a rising exponential function:

$$F(t) = F(1 - e^{-kt}) \tag{5}$$

In Eq. (5), $F$ is the steady-state force approached as $t \to \infty$ and $k$ is the rate of isometric force development for each combination of $K_a$ and $K_{xb}$ and $P_{\mathrm{a}}$. Approximately 1% of parameter estimates for Eq. (5), all at the lowest $P_{\mathrm{a}}$'s, were discarded because the regression either did not converge or because $F$ converged to a value that was substantially higher than $F_{\max}$ (Eq. (6)) due to noisiness of the simulation results at very low activation levels.

For each combination of $K_a$ and $K_{xb}$, $F$ versus $P_{\mathrm{a}}$ results were fit using nonlinear least squares regression (SigmaPlot 2001, SPSS Inc., Richmond, CA) to a modified version of the Hill equation:

$$F = \frac{F_{\max}}{1 + \left(\frac{P_{\mathrm{a}_{50}}}{P_{\mathrm{a}}}\right)^{n}} \tag{6}$$

$F_{\max}$ was constrained to be the average, steady-state force obtained for $P_{\mathrm{a}} = 1.0$. Parameter estimates were obtained for $P_{\mathrm{a}_{50}}$, the value of $P_{\mathrm{a}}$ needed to achieve $F_{\max}/2$, and $n$, which reflects the steepness of the $F$ versus $P_{\mathrm{a}}$ relationship around $P_{\mathrm{a}_{50}}$, and is typically associated with the apparent cooperativity of isometric force development by muscle preparations.

## RESULTS

The output of a series of individual model runs is shown in Fig. 2(A) with $K_{xb} = 1$ pN/nm per cross-bridge, $K_a = 523$ pN/nm per 12.33 nm segment of an actin filament ($a_0$; Methods), and $K_m = 6060$ pN/nm per 14.33 nm segment of a myosin filament ($m_0$; Methods). This value of $K_a$ is 10% of, and $K_m$ is equal to the respective values measured in frog skeletal muscle; $K_{xb}$ is of the same order magnitude measured using single molecule method which provides a lower limit to $K_{xb}$.[21,42,43] Activation probability $P_{\mathrm{a}}$ of thin filament regulatory units was varied between 0.003 and 1.0 and was held constant during each run, which is indicated by different colors in Figs. 2(A) and 2(B). Each simulation was begun with all myosins detached from actin and thus force development started from zero. Figure 2(B) shows an equivalent series of simulations with $K_a$ increased to 52,300 pN/nm (1000% of that measured in frog skeletal muscle). Each force simulation was fit to a rising monoexponential (Eq. (5); black lines in Figs. 2(A) and 2(B)) to obtain steady-state force ($F$) and the rate of tension rise ($k$). Values of $F$ from Figs. 2(A) and 2(B) are plotted as a function of $P_{\mathrm{a}}$ in Fig. 2(C). Figure 2 shows that the dependence of $F$ on $P_{\mathrm{a}}$ is influenced by the stiffness of actin filaments, and that this effect is clearly evident with individual simulations despite the presence of stochastic noise in the model output.

Figure 3 compares a single force simulation with averages of 2–110 simulations using parameters $K_{xb} = 1$ pN/nm, $K_a = 5230$ pN/nm, $K_m = 6060$ pN/nm, and $P_{\mathrm{a}} = 1.0$. A single simulation is shown in Fig. 3(A) along with selected averages of multiple simulations. Steady state $F$ ($\equiv F_{\max}$ because $P_{\mathrm{a}} = 1.0$) for these stiffness values is ~300 pN which is ~1 pN per myosin molecule (not per attached cross-bridge). The model value is thus close to the physiological value of ~1.6 pN per myosin head obtained for frog muscle at 0°C,[2] or in single molecule measurements *in vitro*.[33] All simulations were fit to Eq. (5) and the average, steady state $F_{\max}$ was plotted in Fig. 3(B) (○, gray, open circles); error bars represent SD. The same simulations were averaged and fit to Eq. (5) with the resulting estimates of $F_{\max}$ also plotted in Fig. 3(B) for comparison (□, black open squares); error bars represent SE of regression. Figure 3(B) demonstrates that regression parameters derived from averages of $N$ simulations are indistinguishable from averages of parameters obtained from individual simulations. It also demonstrates that a minimum of 10 Monte-Carlo simulations is necessary for each set of parameters.

Average $F_{\max}$ ($F$ at $P_{\mathrm{a}} = 1.0$) was evaluated for at least 12 simulations when $K_{xb}$ and $K_a$ were varied ($K_a$ values plotted as ratio of 5230 pN/nm). Figure 3(C) shows that $F_{\max}$ varied primarily with $K_{xb}$. $F_{\max}$ also varied with $K_a$ as reported previously for simulations of one actin and one myosin filament,[11] but only at the lowest values of $K_a$ and highest values of $K_{xb}$ examined (Fig. 3(C)). The

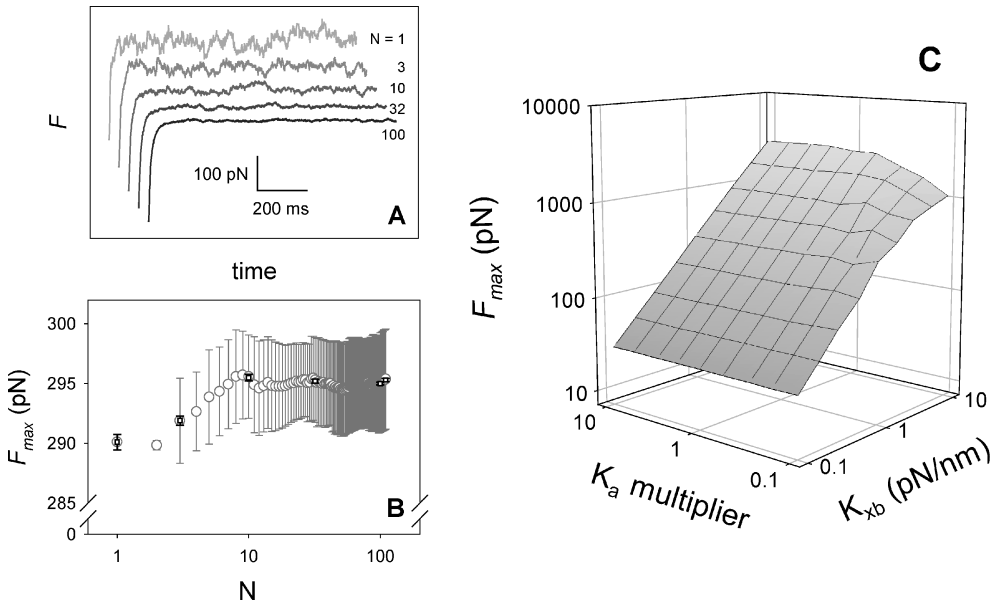


**FIGURE 3. Analysis of steady-state force from multiple simulations. (A) Examples of a single simulation with the average of $N = 3$, 10, 32, or 100 (arranged from lightest and uppermost trace, to darkest and bottommost) simulations of $F(t)$. $P_a = 1.0$, $K_a = 5{,}230$ pN/nm, and $K_{xb} = 1$ pN/nm for all simulations in panels A and B. Simulations were offset on both the time and force axes for clarity. (B) Estimation of steady-state isometric force $F$ (Eq. (5)) from multiple, repeated simulations are shown in panel A. Points are mean $F \pm$ SD averaged from $N$ independent simulations (gray, open circles) and $F \pm$ SE obtained from fits to $N$ averaged simulations (black, open squares). (C) Variation of $F_{max}$ ($F$ for $P_a = 1.0$, as in Eq. (6)) with $K_a$ and $K_{xb}$ in the multifilament model of the sarcomere. $F_{max}$ was calculated as the average of at least 12 independent simulations at $P_a = 1.0$.**

multifilament model results (Fig. 3(B)) suggest that $F_{max}$ may be less susceptible to the presence and amount of filament compliance than the two-filament model that has fewer total cross-bridges and consequently lower $F_{max}$.

Taken together, Figs. 2(C) and 3(C) suggest that filament compliance within the intact sarcomere may be most significant for physiology at submaximal levels of activation ($P_a < 1$). Comparison of $F$ from multiple simulations at two values of actin filament stiffness ($K_a = 5230$ versus 523 pN/nm) when $P_a$ was varied between 0.003 and 1.0 shows a greater effect on submaximal $F$ than on $F_{max}$ (Fig. 4(A)). There are clear differences in the activation-dependence of $F$, here fit by a modified Hill equation (Eq. (6)), even after considering variability encountered due to the stochastic nature of the model. Figures 4(B) and 4(C) illustrate variations in regression parameter estimates for Eq. (6) obtained as illustrated in Fig. 4(A). $K_{xb}$ and $K_a$ were varied ($K_a$ values plotted as a ratio of 5230 pN/nm) over the same ranges and were obtained from the same simulations shown in Fig. 3(C). Figure 4(B) illustrates that the midpoint of activation, $P_{a_{50}}$, is elevated for a range of low $K_a$ and high $K_{xb}$ values. This is equivalent to a decrease in the apparent $Ca^{2+}$-sensitivity of a muscle fiber. Over the same range of parameter values $n$ was decreased, corresponding to a reduction in apparent cooperativity or slope that contributes to and accentuates reduced $Ca^{2+}$-sensitivity of steady-state force. The maximum value of $n$ was $\sim$1, which is consistent with the fact that thin filament regulatory unit cooperativity was explicitly left out of the model.

In addition to steady-state force ($F$), we characterized the rate of force development ($k$ in Eq. (5)) from the simulations (Figs. 2(A) and 2(B)). For constant values of filament and cross-bridge stiffness, average $k$ was plotted as a function of average $F$ obtained by fits to Eq. (5) when $P_a$ was varied (Fig. 5). This approach approximates experimental analysis of the kinetics of tension redevelopment ($k_{TR}$) of permeabilized muscle fibers when $[Ca^{2+}]$ is varied.[4,10,38,41] Figure 5 shows simulations with $K_a = 523$ pN/nm compared with 52,300 pN/nm, values of $K_a$ that correspond to 10 and 1000% of that determined in frog skeletal muscle. The relationships are similar for both values of $K_a$ except at the highest levels of $F$, which correspond to the highest levels of $P_a$. At $P_a = 1.0$, the apparent value of $k$ was slowed to $\sim$40% for $K_a = 523$ pN/nm compared with $K_a = 52{,}300$ pN/nm.

## DISCUSSION

This manuscript describes results of a Monte Carlo, finite element modeling study of biomechanics of a muscle half-sarcomere that includes compliance of the myofilaments. The model was developed to evaluate effects of myofilament compliance on isometric force and incorporated several novel features. All possible cross-bridge

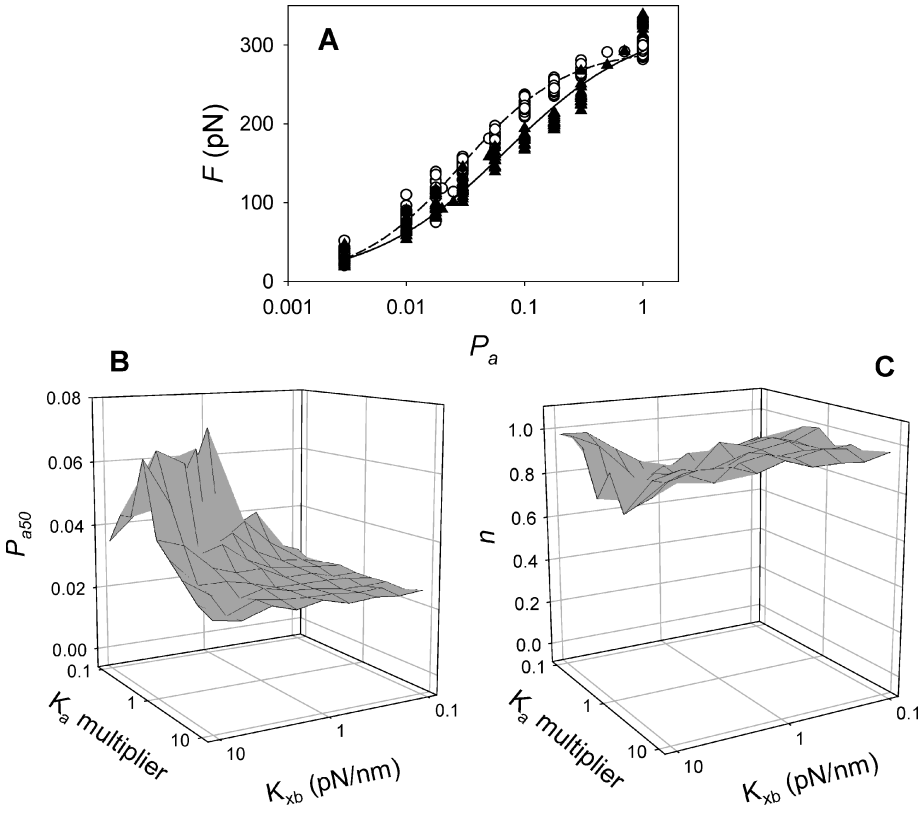


**FIGURE 4. (A) Variation of steady-state force (*F*) with activation level as in Fig. 2(C) except the results from multiple simulations are shown (open circles, $K_a = 5230$ pN/nm; solid triangles, $K_a = 523$ pN/nm). Each point in panel A represents nonlinear least squares regression parameter *F* (Eq. (5)) from a single simulation ($K_{xb} = 1$ pN/nm and $K_m = 6{,}060$ pN/nm). Lines in panel A are nonlinear least squares regression fits to the modified Hill equation (Eq. (6)). (B, C) Variation of Eq. (6) regression parameters $P_{a_{50}}$ (B) and *n* (C) with $K_a$ and $K_{xb}$. Note that the *x*- and *y*-axes were rotated relative to Fig. 3(C). The diagonal ridge in panel B and valley in panel C indicate compliance-dependent changes in all aspects of the apparent activation dependence (both $P_{a_{50}}$ and *n*) of isometric steady-state force.**

interactions were allowable between a thin filament and its surrounding thick filaments, although the number of actual interactions at any given time is severely limited by the geometric constraints of periodic structures of the filaments and structure of the filament lattice. Simulating the probabilistic nature of $Ca^{2+}$ activation, both temporally and spatially, of thin filament regulatory units further modulated the number of cross-bridges. As described previously,[11] cross-bridge cycling was simulated by a thermodynamically correct three-state model. The model executed in reasonable times on a PC which allows wide exploration of parameter space and repeat executions for each set of parameters.

This study was undertaken because compliant realignment of myosin-binding sites on actin was found to modulate isometric force in a two-filament model.[11] The current study was designed to address the specific issues of how this phenomenon is modified when the full complement of filaments, cross-bridges, and force is present. It also asked what additional effects are encountered when the availability of myosin-binding sites on actin is stochastically modulated, as in physiological $Ca^{2+}$-regulation that turns striated muscle contraction on and off. The major findings were as follows: (1) Isometric force in the filament lattice is less susceptible to variations in thin filament compliance than was found previously with a model that included only one thick filament and one thin filament.[11] Force exhibited a clear dependence on cross-bridge stiffness. (2) Activation dependence of steady state, isometric force was influenced by thin filament and cross-bridge compliances. This was reflected by changes in apparent $Ca^{2+}$ sensitivity and apparent cooperativity ($P_{a_{50}}$ and $n$, respectively, in Eq. (6)). (3) Activation-dependence of the rate of tension development was affected by filament compliance. Taken together, these results show that filament compliance could play its most significant role in conditions where muscle activation is submaximal: in cardiac muscle, in skeletal muscle twitches, and perhaps in atrophied conditions.

### *Regulation of Muscle Contraction*

Calcium ions control contractile activity in vertebrate striated muscle by modulating thin filament structure, which alters accessibility of myosin to myosin-binding sites

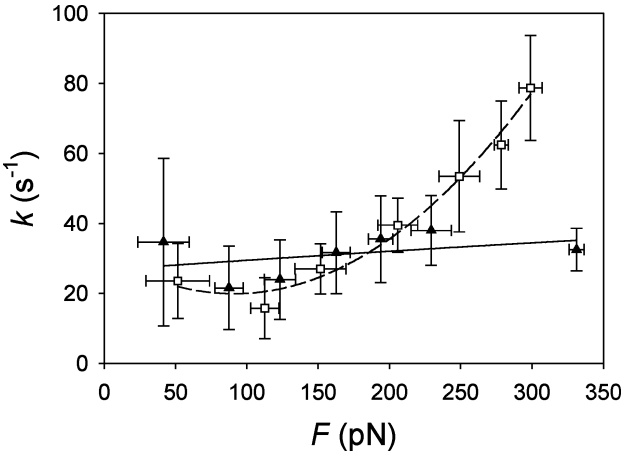


**FIGURE 5. $K_a$ influences the relationship between rate of tension development ($k$) and steady-state isometric force ($F$). Solid triangles, $K_a = 523$ pN/nm; open squares, $K_a = 52{,}300$ pN/nm. Regression parameter estimates for $F$ and $k$ were obtained by fitting Eq. (5) to force simulations when activation probability ($P_a$) was varied between 0.003 (leftmost points for each condition) to 1.0 (rightmost points), as in Figs. 2(A) and 2(B). For each value of $K_a$, regression parameter estimates were combined into 7 bins, equivalent to the procedure applied to $k_{TR}$-force data from muscle preparations. Points are the average ±SD ($N = 11$–21 simulations). Note the similarity between these simulations and $k_{TR}$-force relations obtained from permeabilized muscle fibers when [$Ca^{2+}$] is varied.**

on actin.[17] $Ca^{2+}$ binding to troponin C (TnC) alters protein–protein interactions between subunits of the troponin complex and actin. This in turn allows Tm movement on actin, exposing myosin-binding sites on the thin filament. Our previous two-filament model simulated fully activated muscle filaments although the total force was lower than experienced in the filament lattice of the intact sarcomere. The finding that compliant realignment of binding sites occurred in the low force, two-filament model suggested that submaximal as well as maximum activation levels should be explored in the multifilament model (Fig. 1) with its higher maximum forces. This supposition was corroborated by the finding that myofilament compliance could alter the relation between isometric force and activation level (Fig. 4).

Physiological evidence for a role of CRB in modulating $Ca^{2+}$-activation comes from studies with phalloidin. Phalloidin binding increases the flexural rigidity of actin filaments.[22] In skinned muscle fiber assays, phalloidin increases force at both maximum and submaximal levels of activation.[7] $Ca^{2+}$-sensitivity of skinned bovine ventricular muscle force was increased by ~0.2 pCa units in the presence of phalloidin. Changes in CRB due to increased stiffness can't explain the entire effect of phalloidin, however. $Ca^{2+}$-sensitivity of myofibrillar ATPase, which is measured in the absence of an external load where CRB would be less effective, was also increased but to a lesser extent than force.[6]

Our model utilizes an activation probability ($P_a$) for simulation of the on/off state of thin filament regulatory units. $P_a$ is clearly related to [$Ca^{2+}$], but not linearly. The Monte-Carlo nature of the model was extended to activation of myosin-binding sites on actin to simulate stochastic $Ca^{2+}$ binding to TnC. Cooperative interactions between $Ca^{2+}$-binding sites and between regulatory proteins[17] were omitted from the model to simplify elucidation of filament compliance effects on activation of force. In this situation, activation of neighboring myosin-binding sites is uncorrelated. Further developments of the multifilament model with compliance should include various forms of cooperative interactions that influence thin filament activation.[3,8,17,37] The present study indicates that all aspects of the activation dependence of force could be significantly modulated by filament compliance—a result that was anticipated from results of the two-filament model. The extent of such modulation, however, would depend on the exact form or forms of cooperative coupling that exist in a particular muscle type. There are additional factors that should be considered in models derived from that presented here, including $Ca^{2+}$-dependent changes in compliance of actin filaments, and radial forces that alter filament lattice spacing should also be considered because of their effects on activation of force.[22,32]

### *Kinetics of Force Development*

The rate of tension redevelopment of a muscle fiber following a period of unloaded shortening ($k_{TR}$) has been shown to reflect actomyosin kinetics at maximal $Ca^{2+}$-activation and the dynamics of individual regulatory units at submaximal activation.[10,18,35,36,38] The model simulates tension development from a starting point where no cross-bridges have formed, which corresponds to an idealized $k_{TR}$; the release/restretch maneuvers associated with measuring $k_{TR}$ are intended to forcibly detach as many cross-bridges as possible.[5] Reduction of the maximum rate of tension development in the model, results by 60% for compliant (actin filament stiffness $K_a = 10\%$ of physiological) compared with stiff ($K_a = 1000\%$ of physiological) filaments (Fig. 5), is in general agreement with predictions of lumped parameter models of tension development when series compliance is altered.[27]

There are functionally significant differences in $Ca^{2+}$-activation of $k_{TR}$ between muscle types containing different protein isoforms. Kinetic modeling studies suggested that the shape of the force-$k_{TR}$ relation might reflect isoform differences in $Ca^{2+}$-dependent kinetics of regulatory units turning on and off relative to cross-bridge cycling kinetics.[18] Our model suggests an alternate explanation. A relatively flat $k_{TR}$-force relation, such as found in cardiac muscle,[18] could be due to the presence of more filament compliance than muscles that exhibit steeper force-$k_{TR}$ relations such as fast skeletal muscle.[5,10,35,36,38]

Filament compliance has also been shown to slow the apparent rate of tension transients that occur in response to small amplitude length changes or biochemical perturbations such as rapid increases of Pi.[26,29] This is particularly true at maximum thin filament activation. Tension transients in response to small length changes are faster at submaximal than at maximum levels of thin filament activation, opposite what is observed with tension (re)development kinetics.[28,29] Kinetics of small amplitude tension transients are more likely to reflect cross-bridge kinetics when there are fewer cross-bridges and forces are small, and filament compliance is therefore a less significant variable. This contrasts with $k_{TR}$; physiological data and modeling, including Fig. 5, support the idea that $k_{TR}$ is dominated by thin filament regulatory unit dynamics at subsaturating [$Ca^{2+}$] and thus true actomyosin kinetics would not be extracted without reducing filament compliance.

*Summary*

A computational model was developed that includes compliance of the myofilaments within the structure of the intact filament lattice. Presence of filament compliance could modulate the dependence of steady-state isometric force and the rate of tension development on thin filament activation level. Tuning of biomechanics at the protein level may be as significant at higher levels of organization[13,30] and needs to be considered in biomechanical components of physiological models[24,40,44] to describe changes in muscle associated with exercise and microgravity.[1,39] It is also possible that $Ca^{2+}$-dependent changes in thin filament compliance[22] could play a role in altered $Ca^{2+}$-sensitivity associated with mutations in troponin subunits or Tm that are associated with inherited cardiomyopathies.[14,15,23]

## ACKNOWLEDGMENTS

Support was provided by the National Space Biomedical Research Institute (NASA/NSBRI) MA00211 (PBC); NIH/NHLBI HL63974 (PBC); John D. and Kathryn T. MacArthur Foundation (TLD); Joan and Richard Komen Endowment (TLD); ONR MURI grant (TLD); Mary Gates Endowment (JMM). Dr. Justin R. Grubich assisted in running simulations. The simulation itself benefited greatly from consultation with Drs Daniel Grünbaum, Alan C. Trimble, and Michael S. Tu. We thank Aya Kataoka for critical comments on the manuscript, Sean Burnside and Amanda Clark for technical assistance, and Ken Womble for artwork.

## REFERENCES

[1] Adams, G. R., V. J. Caiozzo, and K. M. Baldwin. Skeletal muscle unweighting: Spaceflight and ground-based models. *J. Appl. Physiol.* 95:2185–2201, 2003.

[2] Bagshaw, C. R. Muscle Contraction. London: Chapman & Hall, 1993.

[3] Brandt, P. W., M. S. Diamond, and F. H. Schachat. The thin filament of vertebrate skeletal muscle co-operatively activates as a unit. *J. Mol. Biol.* 180:379–384, 1984.

[4] Brenner, B. Effect of $Ca^{2+}$ on cross-bridge turnover kinetics in skinned single rabbit psoas fibers: Implications for regulation of muscle contraction. *Proc. Natl. Acad. Sci. U.S.A.* 85:3265–3269, 1988.

[5] Brenner, B., and E. Eisenberg. Rate of force generation in muscle: Correlation with actomyosin ATPase activity in solution. *Proc. Natl. Acad. Sci. U.S.A.* 83:3542–3546, 1986.

[6] Bukatina, A. E., and F. Fuchs. Effect of phalloidin on the ATPase activity of striated muscle myofibrils. *J. Muscle Res. Cell Motil.* 15:29–36, 1994.

[7] Bukatina, A. E., F. Fuchs, and P. W. Brandt. Thin filament activation by phalloidin in skinned cardiac muscle. *J. Mol. Cell. Cardiol.* 27:1311–1315, 1995.

[8] Campbell, K. Rate constant of muscle force redevelopment reflects cooperative activation as well as cross-bridge kinetics. *Biophys. J.* 72:254–262, 1997.

[9] Chase, P. B., M. Macpherson, and T. L. Daniel. A spatially explicit, 3-D model of the muscle sarcomere. *Biophys. J.* 82:5a, 2002.

[10] Chase, P. B., D. A. Martyn, and J. D. Hannon. Isometric force redevelopment of skinned muscle fibers from rabbit with and without $Ca^{2+}$. *Biophys. J.* 67:1994–2001, 1994.

[11] Daniel, T. L., A. C. Trimble, and P. B. Chase. Compliant realignment of binding sites in muscle: Transient behavior and mechanical tuning. *Biophys. J.* 74:1611–1621, 1998.

[12] Daniel, T. L., and M. S. Tu. Animal movement, mechanical tuning and coupled systems. *J. Exp. Biol.* 202 Pt 23:3415–3421, 1999.

[13] Farley, C. T., J. Glasheen, and T. A. McMahon. Running springs: Speed and animal size. *J. Exp. Biol.* 185:71–86, 1993.

[14] Fatkin, D., and R. M. Graham. Molecular mechanisms of inherited cardiomyopathies. *Physiol. Rev.* 82:945–980, 2002.

[15] Gafurov, B., S. Fredricksen, A. Cai, B. Brenner, P. B. Chase, and J. M. Chalovich. The Δ14 mutant of troponin T enhances ATPase activity and alters the cooperative binding of S1-ADP to regulated actin. Biochemistry, In press.

[16] Gittes, F., B. Mickey, J. Nettleton, and J. Howard. Flexural rigidity of microtubules and actin filaments measured from thermal fluctuations in shape. *J. Cell Biol.* 120:923–934, 1993.

[17] Gordon, A. M., E. Homsher, and M. Regnier. Regulation of contraction in striated muscle. *Physiol. Rev.* 80:853–924, 2000.

[18] Hancock, W. O., L. L. Huntsman, and A. M. Gordon. Models of calcium activation account for differences between skeletal and cardiac force redevelopment kinetics. *J. Muscle Res. Cell Motil.* 18:671–681, 1997.

[19] Higuchi, H., T. Yanagida, and Y. E. Goldman. Compliance of thin filaments in skinned fibers of rabbit skeletal muscle. *Biophys. J.* 69:1000–1010, 1995.

[20] Howard, J. Mechanics of Motor Proteins and the Cytoskeleton. Sunderland, MA: Sinaur Associates, 2001.

[21] Huxley, H. E., A. Stewart, H. Sosa, and T. Irving. X-ray diffraction measurements of the extensibility of actin and myosin filaments in contracting muscle. *Biophys. J.* 67:2411–2421, 1994.

[22] Isambert, H., P. Venier, A. C. Maggs, A. Fattoum, R. Kassab, D. Pantaloni, and M.-F. Carlier. Flexibility of actin filaments derived from thermal fluctuations. Effect of bound nucleotide, phalloidin, and muscle regulatory proteins. *J. Biol. Chem.* 270:11437–11444, 1995.

[23]Köhler, J., Y. Chen, B. Brenner, A. M. Gordon, T. Kraft, D. A. Martyn, M. Regnier, A. J. Rivera, C.-K. Wang, and P. B. Chase. Familial hypertrophic cardiomyopathy mutations in troponin I (K183Δ, G203S, K206Q) enhance filament sliding. *Physiol. Genomics* 14:117–128, 2003.

[24]Lambeth, M. J., and M. J. Kushmerick. A computational model for glycogenolysis in skeletal muscle. *Ann. Biomed. Eng.* 30:808–827, 2002.

[25]Linari, M., I. Dobbie, M. Reconditi, N. Koubassova, M. Irving, G. Piazzesi, and V. Lombardi. The stiffness of skeletal muscle in isometric contraction and rigor: The fraction of myosin heads bound to actin. *Biophys. J.* 74:2459–2473, 1998.

[26]Luo, Y., R. Cooke, and E. Pate. A model of stress relaxation in cross-bridge systems: Effect of a series elastic element. *Am. J. Physiol.* 265:C279–C288, 1993.

[27]Luo, Y., R. Cooke, and E. Pate. Effect of series elasticity on delay in development of tension relative to stiffness during muscle activation. *Am. J. Physiol.* 267:C1598–C1606, 1994.

[28]Martyn, D. A., and P. B. Chase. Faster force transient kinetics at submaximal $Ca^{2+}$ activation of skinned psoas fibers from rabbit. *Biophys. J.* 68:235–242, 1995.

[29]Martyn, D. A., P. B. Chase, M. Regnier, and A. M. Gordon. A simple model with myofilament compliance predicts activation dependent cross-bridge kinetics in skinned skeletal fibers. *Biophys. J.* 83:3425–3434, 2002.

[30]McMahon, T. A., and P. R. Greene. The influence of track compliance on running. *J. Biomech.* 12:893–904, 1979.

[31]Mijailovich, S. M., J. J. Fredberg, and J. P. Butler. On the theory of muscle contraction: Filament extensibility and the development of isometric force and stiffness. *Biophys. J.* 71:1475–1484, 1996.

[32]Millman, B. M. The filament lattice of striated muscle. *Physiol. Rev.* 78:359–391, 1998.

[33]Molloy, J. E., J. E. Burns, J. Kendrick-Jones, R. T. Tregear, and D. C. S. White. Movement and force produced by a single myosin head. *Nature* 378:209–212, 1995.

[34]Molloy, J. E., J. E. Burns, J. C. Sparrow, R. T. Tregear, J. Kendrick-Jones, and D. C. S. White. Single-molecule mechanics of heavy meromyosin and S1 interacting with rabbit or *Drosophila* actins using optical tweezers. *Biophys. J.* 68:298S–303S, S–5S, 1995.

[35]Regnier, M., D. A. Martyn, and P. B. Chase. Calmidazolium alters $Ca^{2+}$ regulation of tension redevelopment rate in skinned skeletal muscle. *Biophys. J.* 71:2786–2794, 1996.

[36]Regnier, M., D. A. Martyn, and P. B. Chase. Calcium regulation of tension redevelopment kinetics with 2-deoxy-ATP or low [ATP] in rabbit skeletal muscle. *Biophys. J.* 74:2005–2015, 1998.

[37]Regnier, M., A. J. Rivera, M. A. Bates, C.-K. Wang, P. B. Chase, and A. M. Gordon. Thin filament near-neighbor regulatory unit interactions affect rabbit skeletal muscle steady state force-$Ca^{2+}$ relations. *J. Physiol.* 540:485–497, 2002.

[38]Regnier, M., A. J. Rivera, P. B. Chase, L. B. Smillie, and M. M. Sorenson. Regulation of skeletal muscle tension redevelopment by troponin C constructs with different $Ca^{2+}$ affinities. *Biophys. J.* 76:2664–2672, 1999.

[39]Riley, D. A., J. L. Bain, J. L. Thompson, R. H. Fitts, J. J. Widrick, S. W. Trappe, T. A. Trappe, and D. L. Costill. Decreased thin filament density and length in human atrophic soleus muscle fibers after spaceflight. *J. Appl. Physiol.* 88:567–572, 2000.

[40]Salem, J. E., G. M. Saidel, W. C. Stanley, and M. E. Cabrera. Mechanistic model of myocardial energy metabolism under normal and ischemic conditions. *Ann. Biomed. Eng.* 30:202–216, 2002.

[41]Sweeney, H. L., and J. T. Stull. Alteration of cross-bridge kinetics by myosin light chain phosphorylation in rabbit skeletal muscle: Implications for regulation of actin–myosin interaction. *Proc. Natl. Acad. Sci. U.S.A.* 87:414–418, 1990.

[42]Veigel, C., M. L. Bartoo, D. C. S. White, J. C. Sparrow, and J. E. Molloy. The stiffness of rabbit skeletal actomyosin cross-bridges determined with an optical tweezers transducer. *Biophys. J.* 75:1424–1438, 1998.

[43]Wakabayashi, K., Y. Sugimoto, H. Tanaka, Y. Ueno, Y. Takezawa, and Y. Amemiya. X-ray diffraction evidence for the extensibility of actin and myosin filaments during muscle contraction. *Biophys. J.* 67:2422–2435, 1994.

[44]White, R. J., and M. Averner. Humans in space. *Nature* 409:1115–1118, 2001.